Lagrangian and Eulerian investigation of the flow over periodic hills using advanced PIV and 4D-PTV "Shake-the-box"

A. Schröder[1], D.Schanz[1], D. Michaelis[2], C. Cierpka[3], S. Scharnowski[3] M. Manhart[4] and C.J. Kähler[3]

[1] *German Aerospace Center (DLR), Institute of Aerodynamics and Flow Technology, Department of Experimental Methods, Germany*
[2] *LaVision GmbH, Göttingen, Germany*
[3] *Institute of Fluid Mechanics and Aerodynamics, Bundeswehr University Munich, Germany*
[4] *Institute of Hydrodynamics Technical University Munich, Germany*

andreas.schroeder@dlr.de

1 Introduction

In order to increase the prediction capabilities of advanced numerical methods for high Reynolds number turbulent wall bounded flows highly accurate experimental validation data-sets are strongly required. Sometimes integration times which are necessary for resolving very low frequency flow features like boundary layer superstructures or separation regions due to strong positive pressure gradients are not sufficient for a converged solution. Consequently, the used experimental methods have to be able to resolve a large range of spatial and temporal scales for serving the code validation process. In a joint experiment within the FP7 project AFDAR several advanced particle image velocimetry (PIV) and particle tracking velocimetry (PTV) methods have been successively applied to measure the flow within the the ERCOFTAC test case Nr. 81 "Periodic hill" water tunnel at TU Munich. The periodic hill geometry scales with the hill height h = 50 mm, while the spacing between them was L_x = 9h = 450 mm submerged in the water tunnel facility with a channel height of L_y = 3.035h = 151.75 mm and a width of 900 mm.

Snapshot and time-resolved PIV, using an evaluation scheme based on single-pixel ensemble-correlation, as well as the newly developed high resolution 4D-PTV technique "Shake-the-box" (STB), see Schanz et al. (2013a) have been applied. The STB technique requires a set of time resolved particle images from typically four to six viewing directions similar to time-resolved tomo PIV (Schroeder et al. 2011). The results of the STB evaluation technique are dense, ghostless, highly accurate and nearly complete reconstructions of all particle positions per time step within relatively long Lagrangian tracks. Due to the unique features of this new 4D-PTV technique the focus of the present paper has been put on the description of the STB evaluation technique and demonstrating its capabilities in bridging Lagrangian and Eulerian views of the flow enabling new fluid mechanical insight from combined global and local statistics.

2 Experimental setup and procedures

The tunnel is driven hydrostatically using a water reservoir fed by a pump. The water flow is homogenized by using honey combs and screens installed upstream of the test section. For the current experiment ten hills were arranged in a row and the measurements were performed in the flow around and at the seventh hill, where average periodic flow conditions are developed with respect to the up- and downstream hills. A detailed description of the setup can be found in Rapp and Manhart (2011). The Reynolds number, built with the averaged bulk velocity over the hill crest u_b and the hill height h, was set to Re = 8,000 (u_b = 0.171 m/s) and Re = 33,000 (u_b = 0.698 m/s), respectively.

The first part of the joint PIV experiment was dedicated to a detailed characterization of the overall flow up-, around and downstream of the seventh hill in terms of high resolution 2D mean velocity fields and the corresponding turbulent fluctuations resp. Reynolds stresses by advanced evaluation schemes and statistical methods (see details at Cierpka et al. (2013)). In order to measure the velocity close to the wall, the flow was seeded with Rhodamin B doped polyamide particles with a diameter range of 1-20 µm and the camera was equipped with a low pass light filter. The reflections of the wall were almost completely suppressed by this procedure. To avoid alignment errors the light sheet was generated by a single cavity *InnoLas* laser in double pulse mode. For the image recording a sCMOS camera from *PCO* was operated at 5 Hz for a total measurement time of about 1.2 h for each Reynolds number.

The region downstream of the hill shows large Reynolds stress events and is subject to strong three-dimensional flow features. Therefore, in the second part of the present investigation a camera set-up suitable for time-resolved tomographic PIV measurements have been used while the gained time series of particle images have been evaluated with the novel 4D- PTV technique STB.

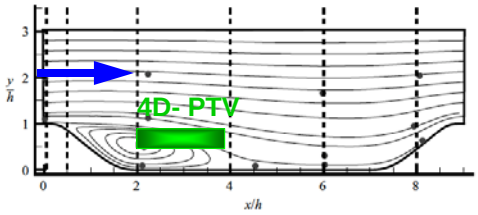

Figure 1: Schematic of the channel with hill (h = 50mm) (test case ERCOFTAC 81) and indicated cross-section of the 4D-PTV measurement volume

Six high speed cameras were used to observe the measurement volume of 90 x 94 x 20 mm^3, located 2 h (100 mm) downstream of the seventh hill. Wall-normal height spans from 25 to 45 mm above the ground wall in order to capture the shear layer (see Fig. 1). The water was seeded using ~30 µm polyamide particles. Illumination was realized using a Nd:YLF Quantronix Darwin Duo high-repetition laser. The laser beam was widened to an oval light profile. The profile was cut in rectangular shape by a passe-partout that was fixed at the side wall of the channel. In order to assure sufficient contrast for the imaged particles, a sheet of black adhesive foil was installed below the illuminated area. Fig. 2 (right) shows the volume light sheet, illuminating the measurement area.

Calibration was done using a 3D-calibration-plate, providing two planes of calibration markers. Small, inevitable errors of the calibration were corrected by applying the method of volume self-calibration to the particle images. Back-projection errors of around 1 pixel were found and corrected to values below 0.02 pixels by this method. In order to allow sufficient seeding densities to resolve small turbulent structures, six high-speed cameras with 4 Megapixels resolution each (Imager pro HS 4M / PCO Dimax) were used to capture time series of particle images (see Fig. 2, left). Three sequences of 3,000 particle images have been achieved at 0.5 kHz frame rate for Re = 8,000 and at 1 kHz frame rate for Re = 33,000 each. All achieved particle images have a density of 0.04 to 0.06 ppp at ~d_p = 3 pixel particle image diameter. An average resolution of 21.5 pixels per mm corresponding to ~46 µm per pixel was achieved, using a 1:1 scaling for the reconstructed measurement volume.

On the one hand the STB algorithm uses a particle image matching procedure based on the iterative particle reconstruction method (Wieneke, 2013) and the determination of the local optical transfer function (OTF) (Schanz et al. 2013b). On the other hand the innovative 4D character of the STB algorithm is relying on the condition that true particles within a volume cannot disappear between time steps. An initialization process is identifying several thousand particle tracks of a certain length and intensity in the first few image samples (which already dramatically reduces the number of ghosts).

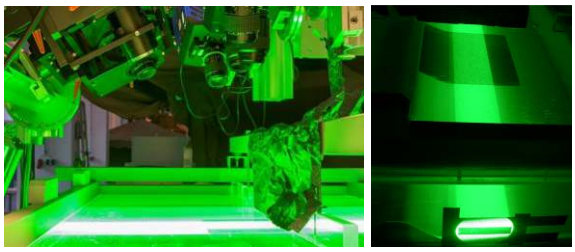

Figure 2: (Left) Six high-speed cameras looking onto the light volume within the periodic hill water flow. (Right) Collimated light volume with ~ 90 x 20 mm² cross-section entering through a passe-partout

Then a growing and further saturating number of particles can be predicted in 3D along all found tracks for time t = n + 1 using a polynomial fitting function, assuming physically reasonable accelerations. The predicted position exhibits already a sufficient accuracy for a next round of the particle image matching scheme. After a few successive time steps the ambiguity of the ill-posed reconstruction problem present for each *single* time step is nearly diminishing in this 4D approach even for high seeding densities up to 0.1 ppp. Further on, only those particles which are newly entering the volume have to be triangulated for some time steps before being tackled by the same scheme. The resulting data are highly accurate long Lagrangian tracks within the reconstructed measurement volume. The reconstruction accuracy of the 3D particle position has been assessed by a simulated STB experiment containing a turbulent flow field in a similar measurement volume. Under ideal imaging conditions an average uncertainty of 0.0033 pixels for particle image densities of 0.05 ppp using four camera projections have been gained, see Schanz et al. (2014). Taking into account the various effects of the present experimental particle imaging properties and vibrations of the single camera lines-of-sight we can conservatively expect a position uncertainty of ~0.05 pixels for the reconstructed particles, which corresponds to ~2.5 µm.

Further on, the particle track data have been fitted by 3rd order polynomials on each of 15 subsequent time steps enabling the determination of e.g. Lagrangian velocities and accelerations. The achieved data-set is unique due to the very high spatial resolution of Lagrangian track data of up to 120,000 particles per time step, treatable as fluid elements with respect to the Kolomogorov scale. Nevertheless, up to the given development point of the STB technique not all tracks which are not physically meaningful can be identified and filtered out during the reconstruction process, which would be the most efficient way to reduce the number of outliers. The problem to tackle is a kind of domino effect, because any reconstructed track, which is not following the true particle path, will affect at least one other track getting biased or even forced to be ended due to missing intensities along the same lines-of-sight in

the residual images. Approximately 5% outliers can be detected in a post-processing step.

3 Results and analysis

For the spatial resolution, the Kolmogorov length scale η can be estimated by taking the value of Breuer et al. (2006) obtained for DNS data at Re = 5,600 and scaling it with $Re^{3/4}$. This results in a mean Kolmogorov length scale for Re = 8,000 of η ~ 100µm and for Re = 33,000 of η ~ 35µm. To increase the spatial resolution for the mean values of the snapshot PIV experiment, the single-pixel ensemble-correlation is required. This technique provides a velocity vector at each pixel location. Nevertheless, the final resolution, i.e. the distance of independent velocity vectors, does strongly depend on the particle image size. The mean particle image diameter was estimated to be 2.4 pixels, which gives a final resolution of 0.45 mm. The mean velocity field is therefore 5 times better resolved than in previous measurements from Rapp and Manhart (2011). A physical spatial resolution of 4.4 η and 12.7 η was achieved for Re = 8,000 and Re = 33,000, respectively.
In Fig. 3 the time averaged velocity field, obtained by single-pixel ensemble-correlation analysis is shown. The acceleration over the hill can be clearly seen. At the hill top a narrow shear layer develops and starts to detach from the hill at x/h = 0.23 for Re = 8,000. Due to the higher momentum the flow follows the contour of the hill and separates further downstream at x/h = 0.31 for the larger Reynolds number. Behind the hill a recirculation zone develops, highlighted by the stream lines.

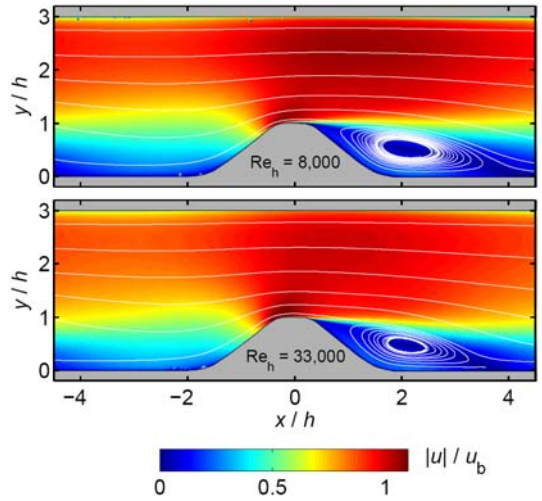

Figure 3: Mean velocity's absolute value fields and characteristic streamlines for Re = 8,000 (top) and Re = 33,000 (bottom).

The STB method allows for the reconstruction of a dense 3D- particle position field along trajectories of the reconstruction scheme enabling an interpolation of the velocity information achieved by the 3rd order polynomial fitting on the Lagrangian tracks. A combined representation of an instantaneous velocity vector field including swirl strength iso-contour surfaces for one time step t = 0 on a regular Eulerian grid from a tomo PIV evaluation together with Lagrangian track data from 20 time steps t = [n-9,…,0,…, n+10] around t = 0 are shown in Fig. 4 (blue arrow indicates the flow direction). One can see the structure arrangement of large-scale high-speed streaks and low speed regions with strong vortices embedded in the shear layers as well as small scale Lagrangian particle motions (vortices) in the low speed regions. In Fig. 5 the magnitude of the Lagrangian acceleration for the same time steps and field of view is colour coded. It is clearly visible that large accelerations are present in the vicinity around the vortex tubes, while in their centre only low acceleration values are present. As vortices in incompressible flows are locations of low pressure values the Lagrangian accelerations around such strong vortices are pointing in average towards the vortex centre. Integrating the Poisson equation along the given data field of material derivatives of the particle velocities (= Lagrangian acceleration) a time-resolved 3D pressure distribution can be calculated as indicated by Liu and Katz (2006).

Furthermore, lower acceleration values are present in the large scale high-speed regions than in low speed regions, especially away from vortices. Within these regions small scale motion together with high values of particle accelerations can be detected which are indicators for strong energy dissipation events. The principal topology of strong dissipative resp. strain regions in shear flow in the vicinity of vortical structures found in Brasseur and Winston (2004) can be confirmed by a first visual inspection of the present data set. Furthermore, the spatial and temporal relation of vortices and Lagrangian acceleration and its role for the momentum transport and turbulence production can be investigated in detail with the given set of data. A statistical investigation by conditional averaging and -space-time-correlations is planned for the future post-processing steps in order to achieve significant topological data involving relevant measures from both frames of reference.

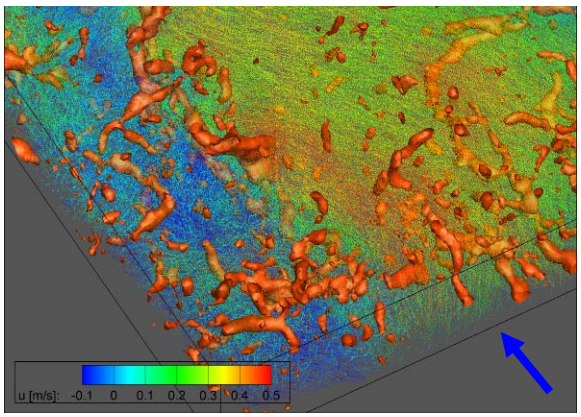

Figure 4: Spatial distribution of Lagrangian tracks (20 time steps) colour coded by u-velocity and related iso-contours of swirl strength λ_2 at Re = 33,000 from Tomo-PIV results at mid time step

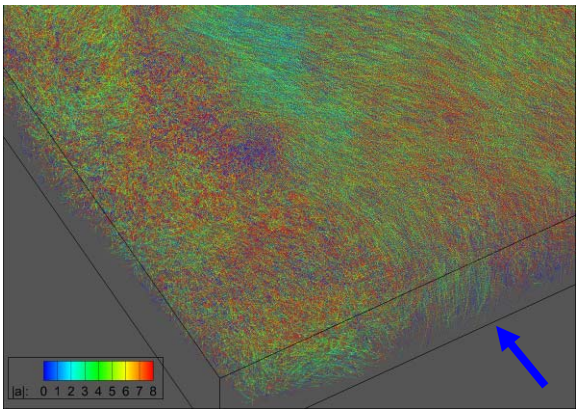

Figure 5: Same Lagrangian particle tracks as in Fig.4 colour coded by the magnitude of acceleration

Furthermore, a detailed analysis of the 3D-vortex dynamics for comparisons with numerical results (Breuer et al. 2009) is foreseen.

For a closer investigation of events involved in turbulence production the data have been used for conditional superposition of Lagrangian tracks with respect to Q2- and Q4-Reynolds stress events, see Bernard and Handler (1990), in order to provide insight into their Lagrangian dynamics. A time series of 200 reconstructed Lagrangian track data have been used for the identification of strong Q2 and Q4-events in subvolumes. The Reynolds decomposition has been realized using a temporal average of all available runs (3 x 3000 time steps) see Fig. 7. Due to the given average flow geometry the turbulence production terms should have been investigated in a coordinate system which is always oriented parallel (for v') and normal (for u') to the curved mean velocity gradients. Here the coordinate system given with respect to the straight wall is used.

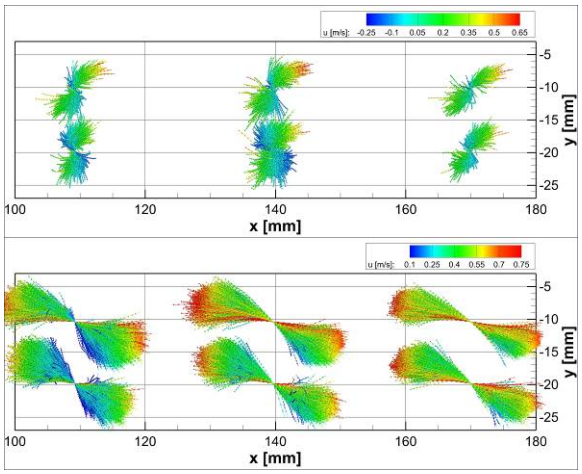

Figure 6: Conditional superposition of Lagrangian tracks (15 time steps back- and forward) of large Q2- (top) and Q4- (bottom) Reynolds stress events > 0.04 m²/s² found in 6 subvolumes within 200 time steps.

In Fig. 6 a set conditionally superimposed Lagrangian tracks found in 6 subvolumes of the investigated flow region is displayed. A value for Q2 and Q4 being larger than -0.04 m²/s² has been searched along all given tracks and the maximum value has been used for fixing each track of the corresponding time step to one point in space. The tracks in Fig. 6 are shown for 15 time steps in back- and forward direction in order to illustrate the dynamics of fluid elements involved in such events. Due to the presence of separated flow regions mainly in the left lower corner of our measurement volume the local spreading of tracks in both temporal directions is governed by the local velocity gradients. It is clearly visible that Q2 events are starting prominently in regions of low velocities and with a larger directional variation of the tracks arbitral in all three dimensions in both temporal directions crossing the fixed Reynolds stress event in comparison to the ones conditioned by large Q4 events. Please not that no relative convection velocity has been subtracted. For the Q2 and Q4 events the spreading of the particle positions before and after several time steps elucidates how fast the conditional Lagrangian correlation function decrease in time. A statistically converged set of conditionally superimposed Lagrangian tracks could help to develop proper RSM turbulence models for RANS.

Each of three time dependent individual runs at 1 kHz has been acquired during 3 sec resulting in 3000 particle images corresponding to 4.653 times flow through from one periodic hill crest to the next based on the bulk velocity u_b = 0.698 m/s at Re = 33.000 which has been defined as a reference t_{ref} in Cierpka et al (2013). The measured Lagrangian tracks of all three runs have been used for a bin-averaging procedure while only tracks with length > 10 were allowed and the first and last two time-steps were not used for enhancing the quality. In total 1.44 * 10^9 data points were distributed to a bin grid of 975 x 202 points with 93 µm (2 vox) bin size in x- and y-directions, while the spanwise z-direction has been projected onto the x-y-plane assuming a converged 2D-flow. Nevertheless, some temporal scales in the measurement volume are of even larger values than 3 sec. The low momentum fluid within the separation bubble located downstream of the hill changes its global shape and spanwise location within the order of several seconds. This fact does not allow to calculate a converged average velocity field out of the present data although a spanwise 2D-projection have been applied introducing a certain amount of statistically independent data due to the lower spanwise coherence length of the involved (small scale) turbulent flow structures. On the other hand, the large scale separated flow regions consist of large spanwise coherence and has an intermittent impact as well in wall normal direction. These findings can be used as a measure for estimating the necessary integration time of time dependent numerical simulations (LES, DNS etc.) aiming at converged flow statistics of the present test case. Beside the discussed convergence problem the bin-average profile of the u-velocity using all three runs together shown in Fig. 7 top fits quite well with the present PIV study using single-pixel-correlation on a large field of view, while for

the latter study the final resolution was estimated by the particle image size to be in the order of 0.45 mm. Additionally, Cierpka et al. (2013) calculated the convergence time t_c/t_{ref} of their approach to be in the order of 40 to several hundred flow through times depending on the local position within the flow.

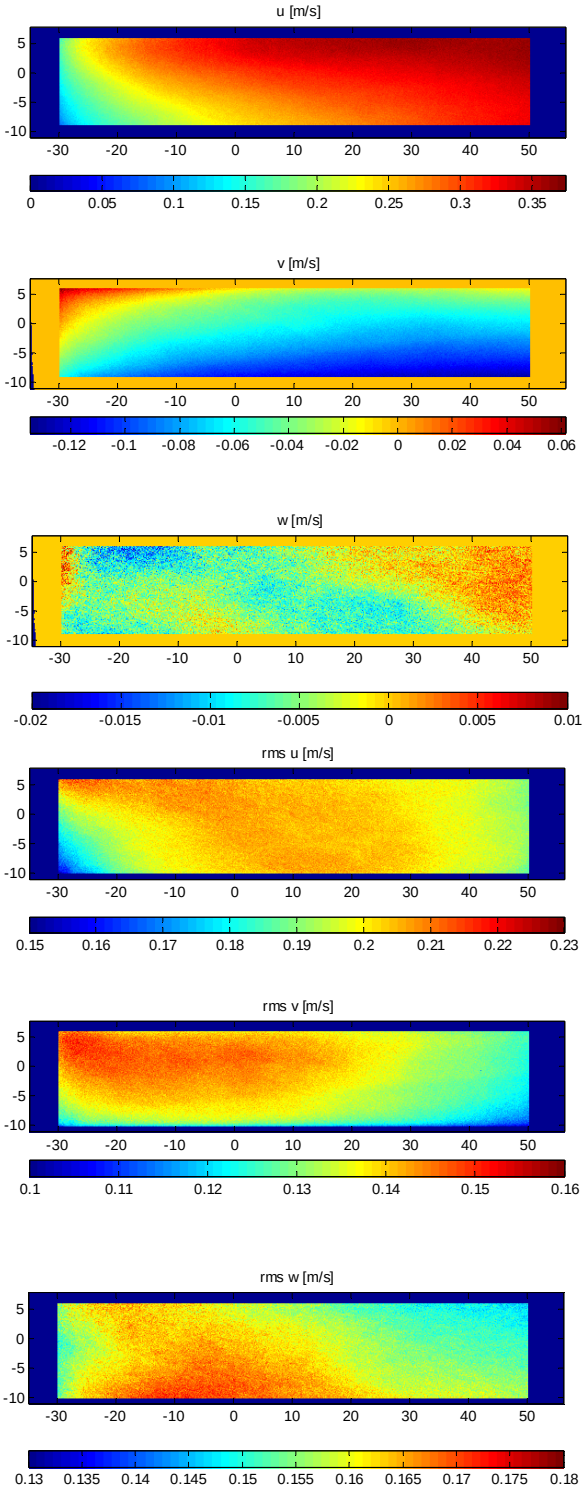

Figure 7: Bin averages (93 x 93 µm² corresponding to 2.65η) of all velocity and rms-fluctuation components based on Lagrangian tracks from 3 x 3000 time dependent runs projected to one plane

In the STB case the spatial resolution was given by two voxels or 93 × 93 µm² bin size, with up to 2700 entries per bin. But this approach would require much more statistically independent data in space and time in order to reach mean flow convergence. In future this goal of accurate Lagrangian track statistics shall be realized using STB on multi-pulse (4 to 8 pulses) 4D-PTV (Schröder et al 2013), which in this study is (partly) given by 500 independent series of 10 time dependent particle image sets for which, due to the limited number of time steps, the STB need to be adapted aiming at a high quality track reconstructions.

In Fig. 7 the corresponding three components of the mean velocity fields are shown in the top three rows. The wall-normal v-velocity shows positive values in the upper left corner due to the presence of the recirculation zone moving tracers upwards at that position, while they are transported in flow direction and downwards following the overall "down-hill" geometry in the rest of the measurement volume. The spanwise w-component of velocity is close to zero which is expected for a mean 2D-flow although the lack of convergence is clearly visible. In the lower three rows of Fig.7 the corresponding rms-values of all three components of the velocity are shown based on the same bin-averaging approach. The rms-values show that the largest contribution to the streamwise turbulent kinetic energy is given in the broadening shear flow along the upper border of the mean recirculation zone, while the largest wall-normal v-velocity contribution is located right below the mean shear region on the left hand side of the volume and covering the upper part of the large u-rms value field on the downstream side of the mean shear. This large region of v-rms velocity values indicate the areas of strong sweeps and ejections organized and accompanied by related vortices aside the low- and high-speed streak formations of the overall turbulent flow which is clearly visible in the instantaneous velocity volumes (see Fig. 4). The w-rms of the spanwise component shows large values in the lower downstream part of the recirculation zone.

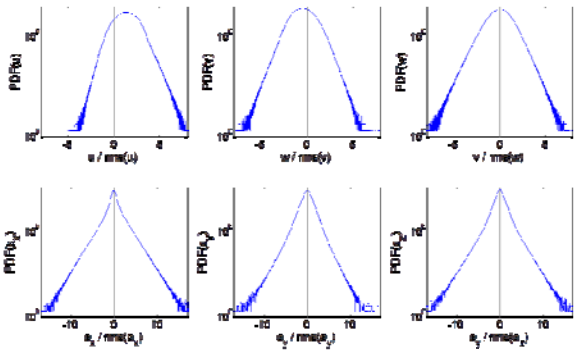

Figure 8: PDFs of the Lagrangian velocity (top) and acceleration (bottom) of all three components normalized by the individual rms-components.

The PDFs of the three components of Lagrangian velocity (Fig. 8 top) shows the mean and dynamic features of the present flow: In the negative u-velocity branch the presence of the recirculation zone is indicated which intermittently increases in wall normal direction at a limited area along the span while it is interrupted as well by the above described large high-speed streaks (see a typical situation in Fig 4). The positive u-velocity covers the majority of the measurement volume while the flat peak is situated at low positive u-velocities. On the positive branch a small shoulder is visible belonging to the typical high-speed streak events in wall bounded turbulence while the corresponding low-speed streak shoulder is hidden from the presence of the recirculation zone. The v-velocity distribution shows a slight overall shift towards negative values due to the known mean flow geometry. The PDF of the spanwise w-velocity is almost symmetric. All three velocities do have a maximum extension of approx. ± 6 respective rms-values.

In Fig. 8 (bottom) the PDFs of the three components of Lagrangian acceleration normalized by its corresponding rms-values are shown. Here the asymmetry and extension of the PDFs toward strong events shall be the main topic. The y-component of the Lagrangian acceleration exhibits the largest asymmetry towards negative values in comparison of the three functions which can be explained on one side by the mean topology of the present shear flow within the measurement volume which consist of mean downward curved streamlines with a recirculation centre right below the left hand corner of the volume. On the other side flow exchange in both shear resp. wall normal directions acts against the mean velocity gradient in positive y-direction which in the majority is resulting in negative y-accelerations for the involved tracers which is well related to the turbulence producing negative Reynolds stress events Q2 and Q4 (see Fig. 6).

3 Conclusions

The examination of the mean velocity, turbulence levels and Reynolds stress distributions indicate that with advanced measurement equipment and sophisticated evaluation techniques all relevant flow features can be resolved. Single-pixel ensemble-correlation on a large number of 2D-PIV data provides the necessary spatial resolution to characterize the flow in a time averaged sense. The newly developed 4D-PTV measurement technique Shake-the-box enables the investigation of spatial and temporal dynamics of coherent structures and Lagrangian particle tracks in the flow region downstream of the 7th hill.

Especially the possibility to achieve a very high spatial resolution for the profiles of the bin-average velocity and Reynolds stress components and the advantages of using the combined data of both Lagrangian and Eulerian reference frames for investigating the role of coherent structures and the dynamics of Lagrangian tracks for turbulence production has been high-lighted. The newly developed 4D-PTV method STB is still under development in order to serve as a reliable Lagrangian tracking technique for future experiments in densely seeded (turbulent) flows.

References

Bernard, P. S., and Handler, R.A. (1990), Reynolds stress and the physics of turbulent momentum transport. *J. Fluid Mech.*, 220: 99-124

Brasseur, J. G and Winston, L. (2005), Kinematics and dynamics of small-scale vorticity and strain-rate structures in the transition from isotropic to shear turbulence. *Fluid Dyn. Res.* 36 357

Breuer, M., Peller, N., Rapp, C., and Manhart, M. (2009), Flow over periodic hills–Numerical and experimental study in a wide range of Reynolds numbers. *Comp Fluids,* 38:433–457.

Cierpka, C., Scharnowski, S., Manhart, M. and Kähler, C.J. (2013), On the significance of high spatial resolution to capture all relevant scales in the turbulent flow over periodic hills, *10th Int. Symp. on PIV*, 1. - 3. 7. 2013, Delft

Fröhlich, J., Mellen, C.P., Rodi, W., Temmerman, L., and Leschziner, M.A. (2005), Highly resolved large-eddy simulation of separated flow in a channel with streamwiseperiodic constrictions. J Fluid Mech 526, 9–66.

Kähler, C.J., Scharnowski, S., and Cierpka, C. (2012). On the resolution limit of digital particle image velocimetry. *Exp Fluids*, 52:1629–1639.

Liu X. and Katz J. (2006) Instantaneous pressure and material acceleration measurements using a four-exposure PIV system , Exp Fluids 41: 227–240, doi 10.1007/s00348-006-0152-7

Rapp, C. and Manhart, M.(2011), Flow over periodic hills: an experimental study. *Exp Fluids*, 51:247–269.

Schanz, D., Schröder, A., Gesemann, S., Michaelis, D., Wieneke, B. (2013a), 'Shake The Box': A highly efficient and accurate Tomographic Particle Tracking Velocimetry method using prediction of particle positions, *10th Int. Symp. on PIV*, 1. - 3. 7. 2013, Delft

Schanz D, Gesemann S, Schröder A, Wieneke B, Novara M (2013b) Non-uniform optical transfer functions in particle imaging: calibration and application to tomographic reconstruction, Meas. Sci. Technol. 24 024009

Schanz D, Gesemann S, Schröder A (2014)" 'Shake The Box' - a 4D PTV algorithm: Accurate and ghostless reconstruction of Lagrangian tracks in densely seeded flows", 17th International Symposium on Applications of Laser Techniques to Fluid Mechanics, Lisbon, Portugal, 07-10 July, 2014

Schröder A, Schanz D, Geisler R, Willert C, Michaelis D (2013) Dual-Volume and Four-Pulse Tomo PIV using polarized laser lights, 10th Int. Symp. on Particle Image Velocimetry – PIV13, 01. - 03. Jul. 2013, Delft, The Netherlands.

Schröder, A., Geisler, R., Staack, K., Elsinga, G., Scarano, F., Wieneke, B., Henning, A., Poelma, C., Westerweel, J. (2011), Eulerian and Lagrangian views of a turbulent boundary layer flow using time-resolved tomographic PIV. *Exp Fluids* 50: 1071-1091

Wieneke, B. (2013), Iterative reconstruction of volumetric particle distribution, *Meas. Sci. Technol.* 24 024008